MODELLING OF IN-PLANE LOADED CLAY UNIT MASONRY WALLS

F. da PORTO[1], G. GUIDI[2], E. GARBIN[3], C. MODENA[4]

[1]Assistant Professor; [2]Engineer; [3]PhD Student; [4]Full Professor
Dept. of Structural and Transportation Eng.
University of Padova,
Via Marzolo 9, 35131 Padova, Italy
daporto@dic.unipd.it

SUMMARY

An extensive experimental research aimed at defining the mechanical behaviour, under in-plane actions, of perforated clay unit load bearing masonry walls, built with different typologies of head and bed joints, has been recently carried out at the University of Padua. Based on the experimental results, a numerical research aimed at investigating the behaviour of the three tested masonry typologies and the reliability of four different modelling strategies to simulate the types of tests, was carried out. In the present contribution, the results of the finite element analyses are discussed.

INTRODUCTION

Development in the masonry industry and in the construction sector imposes the use of different typologies of clay unit, assembled with different types of head and bed joints. The various types of masonry are recognized by the Eurocode 6 (EN 1996-1-1, 2005) but, traditionally, only the construction of masonry made with filled head joints has been allowed in seismic zones. However, the latest version of the Eurocode 8 defers the permission of their use in seismic areas to each country (EN 1998-1, 2004). For this reason, the investigation into the mechanical behaviour and the characteristics of masonry made with different kinds of units, joints and bonding arrangement, still constitutes a topic of interest, as demonstrated by some recent extensive experimental researches (Tomaževič et al., 2006). Furthermore, despite great advances have been made in the modelling of masonry structures (Rots, 1997), the definition of adequate modelling strategies for masonry is still a difficult task.
In this framework, an extensive experimental campaign was carried out in order to characterize the mechanical behaviour of perforated clay unit load bearing masonry walls. Fifty-one specimens were characterized by means of uniaxial and diagonal compression tests and by means of in-plane cyclic shear compression tests. Three types of masonry walls were investigated, namely masonry made with unit with mortar pocket (in the following referred to as Po), masonry made with tongue and groove units (TG), masonry made with unit with small dimensional tolerance in height and thin layer mortar (TM). The results of the experimental campaign are presented in (da Porto et al., 2005).
Four types of non-linear finite element models were used in order to simulate the experimentally observed behaviour. Both macro-modelling and micro-modelling strategies were adopted. Two types of material constitutive laws were implemented in each of the modelling strategies. Isotropic total strain rotating crack model (Rots, 1997) and orthotropic plastic model that uses a Rankine-Hill failure criterion were adopted (Lourenço et al., 1997).

From the comparison of the obtained results, it was possible to draw some conclusions about the adopted experimental procedures, the different behaviour of the three masonry typologies and the reliability of the different modelling strategies to simulate the different types of tests. It was also possible to carry out some parametrical analysis.

EXPERIMENTAL PROGRAM AND NUMERICAL MODELLING

The experimental phase started with almost 150 tests made on mortars and units. Subsequently, 70 tests on micro-assemblages for the determination of the properties of the unit-mortar interface (couplets and crossed couplets) and 51 tests on large masonry assemblages were carried out. The latter included uniaxial compression tests, diagonal compression tests and shear compression tests. A summary of the experimental results can be found in (da Porto et al., 2005).
The experimental results were reproduced by means of both macro-modelling and micro-modelling strategies. Two types of material constitutive laws were implemented in the continuum model. The isotropic total strain rotating crack model (TSRCM) is simple but adequate to reproduce also the secant unloading branch. The second adopted model is the orthotropic plastic model that uses a Rankine-Hill failure criterion, developed by (Lourenço et. al., 1997). The micro-modelling strategy has been based on a simplified model with continuum elements for the units and an interface element to represent the mortar joint and its area of adhesion to the units. The interface behaviour is described by a Coulomb friction criterion with parabolic compression cap and a tension cut-off (Lourenço and Rots, 1997).
The analyses were carried out using the code DIANA™ release 9 (2005). Eight-node plane stress distribution elements with Gauss integration scheme were used in the models, and six-node interface elements with Lobatto integration scheme were adopted for the interfaces in the micro-models. The Newton-Raphson iteration procedure was used with an arc-length control and an energetic convergence criterion. Table 1 gives a short overview of the experimental tests carried out and the corresponding analyses performed.

Table 1. Tests carried out on masonry assemblages and modelling strategies adopted.

Type of unit	Type of test	Number of tests	Type of modelling
TM; TG (& Po)	Sliding along the bed joint	9; 9 (+9)	None
TM; TG (& Po)	Tensile strength along the bed joint	6; 6	None
TM; TG; Po	Uniaxial compression	6; 6; 6	Continuum TSRCM; Continuum Orthotropic; Micromod. TSRCM; Micromod. Orthotropic
TM; TG; Po	Diagonal compression	6; 6; 6	
TM; TG; Po	Shear compression tests	5; 5; 5	

CALIBRATION OF THE PROPOSED MODELS

Various criteria have been proposed for the calibration of the numerical models.
The fracture energy of masonry in tension (G_f^I) and in compression (G_c) are the only parameters needed into the continuum model implementing the isotropic total strain rotating crack constitutive law that have not been experimentally evaluated. These values have been found by means of extensive research on the literature, summarized into a data base valid for

masonry structures (Guidi, 2006) and also on the basis of the values and the equation proposed for concrete by the "Model Code 90", as suggested by (Lourenço, 1996).
The orthotropic plastic continuum model that uses the Rankine-Hill failure criterion needs more parameters. The elastic modulus in the horizontal direction E_x has been evaluated on the basis of the ratio of the net areas in the two orthogonal directions (equation 1):

$$E_x = E_y \cdot \left(\frac{A_{net,x}}{A_{net,y}} \right) \quad (1).$$

According to the results obtained by means of the crossed-couplet test of tension along the bed joint, where the collapse mechanism involved the mortar dowels in the unit holes, the tensile strength in the vertical direction f_{ty} was close to the tensile strength of the bedding mortar f_t on the net area of the holes. The tensile strength of the mortar f_t has been evaluated by reducing by 10% the tensile strength of the mortar in flexure $f_{t,fl}$, according to the Eurocode 2 (EN 1992-1-1, 2004). For evaluating the tensile strength f_{tx} and the compressive strength f_{cx} of masonry in the horizontal direction, the same procedure explained for the elastic modulus was adopted (equation 1). The fracture energy of masonry in tension and in compression in the two directions and the parameters α, β and γ that define the envelope of the Rankine-Hill failure criterion were determined according to the values proposed by (Lourenço 1996). Table 2 gives the parameters adopted into the orthotropic continuum model. From the values given for the y-direction in this table, it is possible to infer also the corresponding parameters of the isotropic total strain rotating crack model.
The homogenization procedure leads to the definition of the linear stiffness k_n and k_s of the mortar joints, which are needed in the interface model. The classical formulation for the homogenization that can be found in literature, leads to an overestimation of the stiffness values. The latter are generally reduced to carry out the analysis (Rots, 1997). In the present study, the homogenization has been carried out on the basis of the equivalence between the experimental displacement (Δl_{exp}), the elastic material displacement (Δl_{tot}) and the model displacement ($\Delta l'_{tot}$). The first is the displacement measured during the experimental compression test and is related to a global experimental elastic modulus E_{exp}. The elastic material displacement can be seen as the sum of the ideal elastic displacement in the unit and in the mortar (L), related to the corresponding elastic moduli E_u and E_m, plus a correction (Δ) due to the behaviour of the interface between the mortar joint and the unit. Finally, the model displacement can be seen as the sum of the displacement in the homogenized unit, related to the corresponding homogenized unit height h'_u and elastic modulus E'_u, and the displacement in the interface related to the corresponding interface stiffness k_n.
From the equivalence $\Delta l_{exp} = \Delta l_{tot} = \Delta l'_{tot}$ and by assuming that the correction in the elastic moduli of the unit and the mortar is reciprocally proportional to the ratio of the corresponding displacement to the elastic material displacement, it was possible to obtain the homogenized elastic moduli of the unit E'_u (equation 2) and of the mortar E'_m (equation 3) and the interface stiffness k_n (equation 4):

$$E'_u = \frac{h_u}{\left[\frac{h_u}{E_u} + \left(\frac{\Delta}{L} \cdot \frac{h_m}{E_m} \right) \right]} \quad ; \quad E'_m = \frac{h_m}{\left[\frac{h_m}{E_m} + \left(\frac{\Delta}{L} \cdot \frac{h_u}{E_u} \right) \right]} \quad (2; 3)$$

Table 2. Parameters of the orthotropic continuum model. The parameters of the isotropic total strain rotating crack model can be obtained from the values in the y-direction.

Unit	E_x [N/mm^2]	ν -	f_{tx} [N/mm^2]	G_{fx}^I [N/mm]	f_{cx} [N/mm^2]	G_{fcx} [N/mm]	α -	γ -
TM	3191	0.45	0.177	0.018	4.93	17.03	0.71	2.13
TG	3143	0.36	0.158	0.018	3.62	16.51	0.64	1.91
Po	3185	0.25	0.167	0.018	4.93	16.36	0.61	1.82
	E_y [N/mm^2]	G_{xy} [N/mm^2]	f_{ty} [N/mm^2]	G_{fy}^I [N/mm]	f_{cy} [N/mm^2]	G_{fcy} [N/mm]	β -	κ_p [10^{-3}]
TM	4497	1551	0.249	0.018	6.95	17.81	-1	0.65
TG	4924	1810	0.247	0.018	5.67	17.32	-1	1.05
Po	5237	2095	0.274	0.018	6.95	17.19	-1	1.18

Table 3. Parameters of the orthotropic micro-model. The parameters of the isotropic total strain rotating crack micro-model can be inferred by this table (same values for the interfaces, same values for the unit in the y-direction)

unit	E_x [N/mm^2]	ν -	f_{tx} [N/mm^2]	G_{fx}^I [N/mm]	f_{cx} [N/mm^2]	G_{fcx} [N/mm]	α -	γ -
TM	6615	0.22	0.332	0.024	7.57	17.03	0.71	2.13
TG	5104	0.17	0.300	0.022	9.10	16.51	0.64	1.91
Po	4797	0.14	0.352	0.025	7.95	16.36	0.61	1.82
	E_y [N/mm^2]	G_{xy} [N/mm^2]	f_{ty} [N/mm^2]	G_{fy}^I [N/mm]	f_{cy} [N/mm^2]	G_{fcy} [N/mm]	β -	κ_p [10^{-3}]
TM	9269	3799	0.468	0.034	20.42	17.81	-1	0.90
TG	7767	3319	0.472	0.034	20.96	17.32	-1	0.36
Po	7704	3379	0.579	0.042	20.43	17.19	-1	0.45

Bed joint interface	k_n [N/mm^3]	k_s [N/mm^3]	f_t [N/mm^2]	f_c [N/mm^2]	G_f^I [N/mm]	G_{fc} [N/mm]
TM	34.90	14.42	0.36	25	0.026	20
TG	57.13	24.88	0.89	25	0.050	20
Po	69.46	30.17	0.89	25	0.063	20
	c [N/mm^2]	**tgφ** -	**tgψ** -	C_s -	G_f^{II} [N/mm]	κ_p [10^{-3}]
TM	0.440	0.400	0	16	0.044	1.40
TG	0.900	0.640	0	16	0.090	0.34
Po	0.900	0.64	0	16	0.090	0.67
Head joint interface	k_n [N/mm^3]	k_s [N/mm^3]	f_t [N/mm^2]	f_c [N/mm^2]	G_f^I [N/mm]	G_{fc} [N/mm]
TM	25.10	10.36	0.021	11	0.000018	19.29
TG	33.00	14.34	0.00022	11	0.000018	19.29
Po	38.20	16.62	0.21	11	0.018	19.29
	c [N/mm^2]	**tgφ** -	**tgψ** -	C_s -	G_f^{II} [N/mm]	κ_p [10^{-3}]
TM	0.044	0.0875	0	16	0.0044	0.42
TG	0.054	0.0875	0	16	0.0054	0.86
Po	0.360	0.64	0	16	0.036	1.04

$$k_n = \frac{1}{\left[h_u^{'}\left(\frac{1}{E_{\exp}} - \frac{1}{E_u^{'}}\right)\right]} = \frac{E_u^{'} \cdot E_m^{'}}{\left[h_m \cdot \left(E_u^{'} - E_m^{'}\right)\right]} \quad (4)$$

The same procedure can be used for the evaluation of the homogenized shear moduli and the corresponding k_s. The other parameters needed for the definition of the failure criterion have been chosen according to the literature (Rots, 1997; Lourenço, 1996) and the values of fracture energy have been fixed also on the basis of the compiled catalogue (Guidi, 2006). The interface model requires the use of the experimentally evaluated parameters for the mortar and the units, and does not rely on the values obtained on the masonry walls.
The orthotropic micro-model adopts the same criteria for the definition of the interface properties, whereas the properties of the orthotropic unit are obtained on the basis of the ratio of the net areas in the two orthogonal directions, by applying the general criterion expressed for the elastic moduli by equation (1). Table 3 gives the parameters adopted into the orthotropic micro-model. The parameters which are implemented in the corresponding micro-model with the isotropic total strain rotating crack constitutive law can be inferred by this table. From the values given for the unit in the y-direction it is possible to infer the values for the isotropic unit, whereas the same values were adopted for the interfaces.

UNIAXIAL AND DIAGONAL COMPRESSION

The analyses of the uniaxial compression tests carried out on the three masonry typologies gave similar results, apart from the continuum model that implements the total strain rotating crack costitutive law. The latter is not able to reproduce the behaviour of the masonry walls till the ultimate state, while the others models are able to reproduce very well both the value of the experimental ultimate load (see Table 4) and the deformability characteristics along the loading direction.

Table 4. Uniaxial compression, experimental ($P_{u,e}$) and numerical ($P_{u,m}$) ultimate load.

Masonry typology	**Mean experimental**	**Continuum Orthotropic**		**Continuum TSRCM**		**Micro-model Orthotropic**		**Micro-model TSRCM**	
	$P_{u,e}$ [kN]	$P_{u,m}$ [kN]	$P_{u,e}/P_{u,m}$ %	$P_{u,m}$ [kN]	$P_{u,e}/P_{u,m}$ %	$P_{u,m}$ [kN]	$P_{u,e}/P_{u,m}$ %	$P_{u,m}$ [kN]	$P_{u,e}/P_{u,m}$ %
TM	2050.1	2035.8	99.3	1306.8	63.7	2041.2	99.6	2046.6	99.8
TG	1686.0	1674.0	99.3	1306.8	77.5	1679.4	99.6	1684.8	99.9
Po	1583.2	1576.8	99.6	1252.8	79.1	1587.8	100.3	1587.6	100.3

The vertical displacements (negative in Figure 1a) are generally better reproduced for the specimens TG and Po, whereas the models of the thin layer joint specimens are stiffer than the real walls. The horizontal displacements (positive in Figure 1a) are well estimated for the three masonry typologies up to the opening of the first crack, above this they are undersized. The continuum orthotropic model is the only one which is able to meet the trend of the horizontal displacements before and after the crack opening (see Figure 1a).
The experimental evidence confirms that all the models show the concentration of stresses induced by the test set-up in the centre of the specimens. The main difference in the behaviour of the three tested masonry typologies is related to the presence of the vertical mortar joint in the specimens Po. This produces a better distribution of the tensile stresses due to the

compression. However, due to the higher tensile stresses that the filled head joints can transfer to the units, this results into a decrease of the ultimate load (see Figure 2). According to the experimental evidence this particular behaviour, could be highlighted only by the micro-models. On the contrary, no particular differences could be highlighted between the behaviour of ordinary (TG) and thin layer (TM) bed joint masonry made with tongue and groove units.
The analyses of the diagonal compression tests carried out on the three masonry typologies gave different results. The continuum models bring a significant overestimation of the ultimate load (see Figure 1b). The presence of unfilled head joints in the masonry specimens TG and TM, yields to a distribution of principal stresses which is quite different from those predicted by the continuum material, which can be identified only by means of the micro-models (see Figure 3). The principal stresses, are not homogeneously distributed, but are concentrated in parallel diagonal bands.

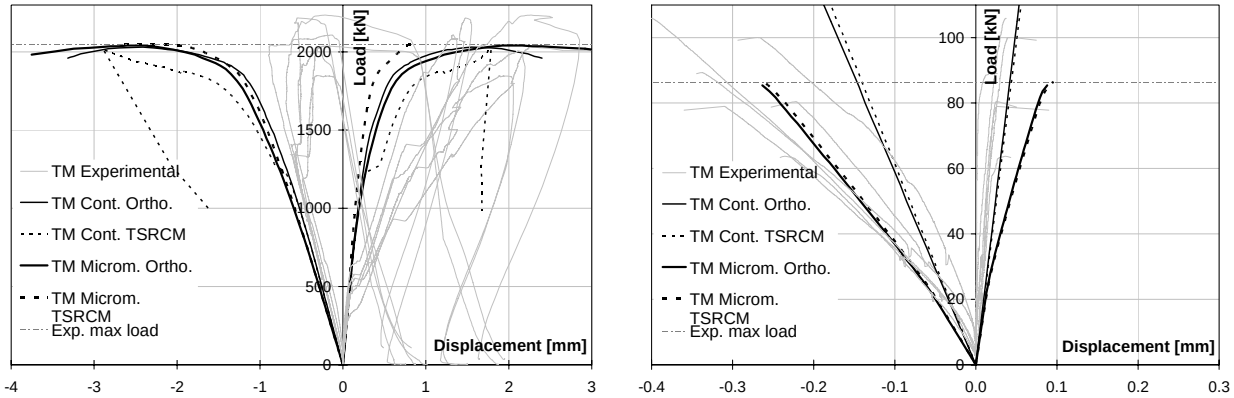

(a) (b)

Figure 1. Experimental and numerical load-displacement diagrams for the specimens TM. Uniaxial compression (a); diagonal compression (b).

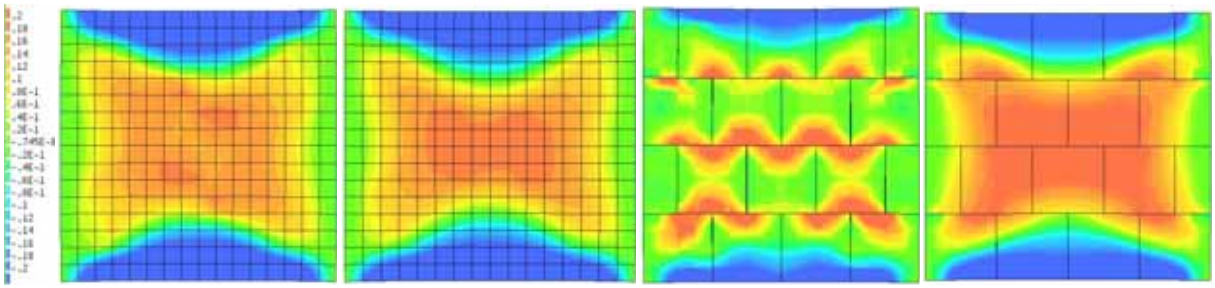

(a) (b) (c) (d)

Figure 2. Principal tensile stresses at 50% of the ultimate load. Orthotropic continuum model: (a) TM, (b) Po; interface model with orthotropic units: (c) TM, (d) Po.

This distribution is favoured by the unit geometry (shape and dimension), by the masonry texture (one layer masonry with simple overlap), and by the presence of the unfilled head joints. The stress bands follow the masonry texture and not the main geometric diagonal of the masonry wall, therefore the areas close to the head joints are almost unloaded (Figure 3).
In terms of both ultimate load and stiffness, the micro-models generally show a good agreement to the experimental behaviour. The fact that the experimental horizontal displacements are lower than the numerical ones, can be also explained due to the small entity of these displacements, which are characterized by magnitude similar to the measuring device sensitivity. The experimental load-displacements curves present a discontinuity between 20 and 40 kN, due to the first settling of the joints. In the same range of load, the micro-models show a decrease of the stiffness.

The collapse occurs, both in the experimental evidence and in the micro-models, due to a tensile stresses concentration in the bed joints, which is maximum in the second mortar joint around the central unit. The failure there is initially located, followed then by the failure of the lower and the upper joint along the same direction, with the separation of the specimen into two portions (Figure 3). The models confirm the fragility of the collapse mode, and highlight the inadequacy of the diagonal test set-up to study the shear behaviour of large unit masonry walls.

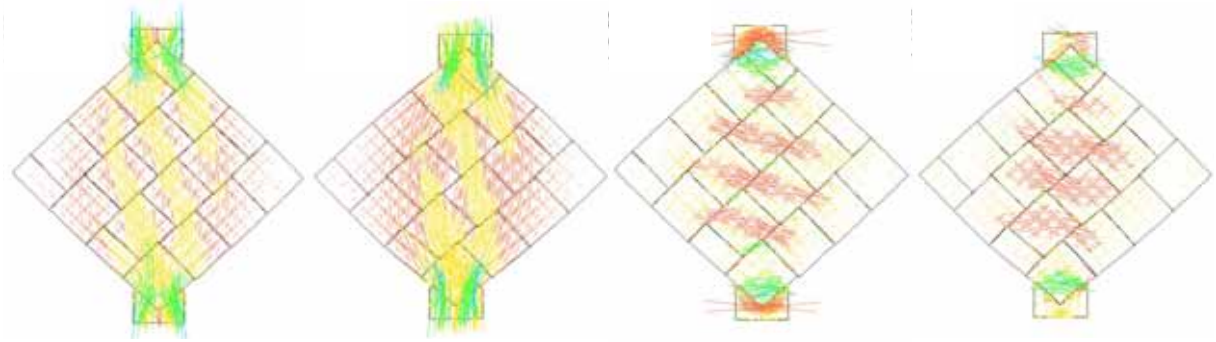

(a) (b) (c) (d)

Figure 3. Interface model with orthotropic units. Principal compression stresses at the ultimate load: (a) TM, (b) Po; principal tensile stresses at the ultimate load: (c) TM, (d) Po;

SHEAR-COMPRESSION TESTS

The shear compression tests were carried out on specimens having cantilever type boundary condition, with fixed base and top end free to rotate, by applying a centred and constant vertical load equal to 17%, 21%, 27% and 33% of the measured maximum compressive strength. Horizontal cyclic displacements, with increasing amplitude and with peaks repeated three times for each displacement amplitude, were applied at a frequency of 0.004 Hz.

The continuum models are very sensitive to the parameters defining the tensile strength and, in fact, they presented an anticipated failure that also modified the sequence of the observed damage mechanisms. Both for isotropic and orthotropic models to avoid this inconvenience, the highest values of tensile strength, i.e. f_{ty}, have been used. This allowed to re-establish the correct sequence of damage mechanisms and to obtain values of ultimate horizontal load in agreement to the experimental ones. Furthermore, due to the concentration of stresses in the compressed toe of masonry and to avoid the anticipate collapse in the numerical simulation, it was necessary to raise the compressive strength values f_c towards the values adopted for the unit strength in the micro-models. The micro-model that implements the total strain rotated crack model for the units, were able to reproduce fairly good the experimental behaviour without any correction of the parameters extracted from the experimental characterization, and used for the analysis of the specimens under uniaxial and diagonal compression.

On the contrary, the orthotropic continuum model and interface model, that implements the Rankine-Hill constitutive law, were inadequate to reproduce the experimental behaviour. The iterations stopped at a displacement and load level definitely lower compared to the real ones. Finally, in all the analysed cases, all the models were able to reproduce very well the initial elastic stiffness of the specimens. In particular, the continuum models, always gave stiffer results when compared to the micro-models.

Figure 4 shows, for the three masonry typologies, a comparison between the experimental behaviour, represented by the envelope of the hysteresis loops (grey colour), and the numerical results. The comparison is carried out for the specimens tested under a compressive

load equal to 22% and 27% of their compressive strength. The isotropic models, which gave the best results, reproduced very well the stiffness and the maximum horizontal load, which was only slightly underestimated. However, they were not able to follow the displacement up to the maximum value at collapse. The isotropic micro-models were able to estimate the maximum load with an average error of about -5% and the maximum displacement with an error of -15%, except for the case of the specimens Po (+15%).

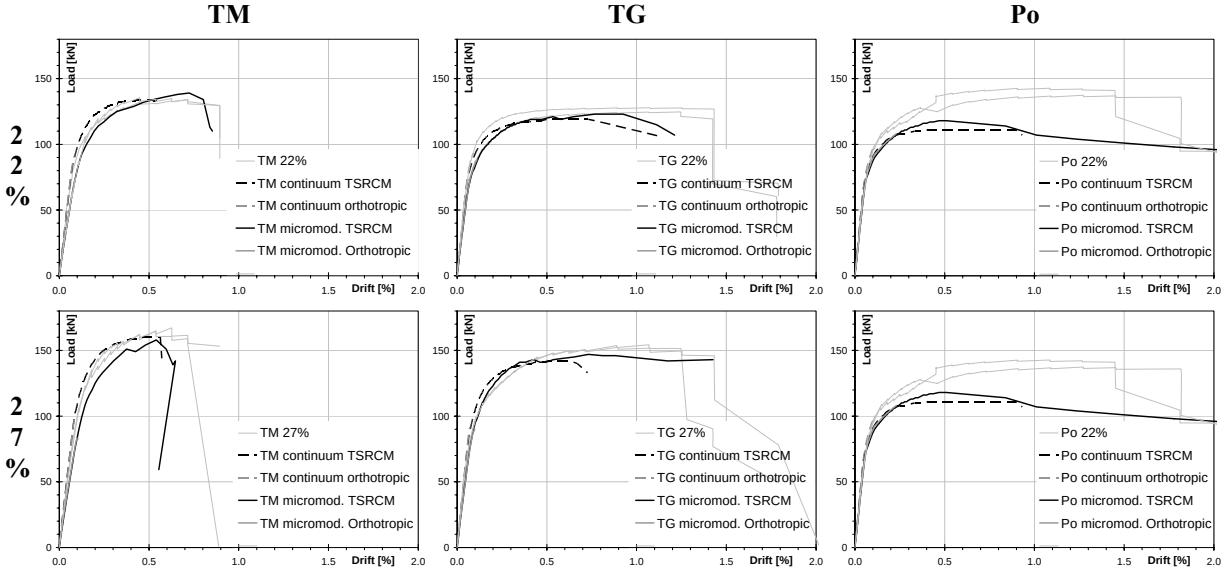

Figure 4. Load-drift diagrams. Experimental behaviour (grey), continuum models (dash line), micro-models (full line), isotropic model (black), orthotropic model (red).

PARAMETRIC ANALYSES

From the obtained results, it appeared that the simplified micro-modelling strategy, with the total strain rotating crack law for the unit, is the most adequate to reproduce monotonically the cyclic shear behaviour of masonry. Therefore, this model was used to carry out parametric analyses of the tested masonry typologies, in order to investigate the influence of the unit compressive strength (f_{cu}) on the global shear behaviour of the tested specimens. The real perforated clay units had a compressive strength of about 20 N/mm^2, the analyses were repeated using units characterized by a compressive strength equal to 15 and 10 N/mm^2. The elastic moduli E_u of the modelled units have been defined on the basis of the unit compressive strength, according to equation (5), which was defined on the basis of an extensive research on literature and the creation of a data base of unit properties:

$$E_u = 3041 f_{cu}^{0.333} \quad (5).$$

For the estimation of the unit tensile strength (f_{tu}) the formulation proposed by the EC2 (EN 1992-1-1, 2004) has been adapted to the following equation (6):

$$f_{tu} = 0{,}9(0{,}3 f_{cu}^{0.58}) \quad (6).$$

The compressive strength of masonry f_c was estimated on the basis of equation (7), where f_m is the mortar compressive strength. This equation was also obtained by calibrating an existing

formulation, and by cataloguing and interpolating results about different typologies of clay unit masonry found in literature (Mosele, 2004):

$$f_c = \frac{f_{cu}}{4{,}25}\log(f_m + 2{,}75) \quad (7).$$

Figure 5 shows, for the three masonry typologies, a comparison between the experimental behaviour (grey) and the numerical results of the isotropic micro-model (black), under a compressive load equal to 22% and 27% of the masonry compressive strength. In the same diagrams, the load-drift curves corresponding to units with compressive strength equal to 15 N/mm^2 (blue) and equal to 10 N/mm^2 (red) are represented. The analyses were carried out by applying the same vertical load (dash line) or a vertical load corresponding to the same ratio (22% and 27%) between the applied load and the compressive strength of masonry.
In the first case, the strength shows a decrease of about -5% and -11% for the masonry type TM, of about -2% and -7% for the masonry types TG and Po, but in particular the masonry presents a strong decrease of the maximum displacement (about -14% and -27% for the masonry type TM, of about -20% and -40% for the masonry types TG and Po). In the second case, it is possible to better appreciate the effect of the unit strength. In the case of the masonry specimens TM, the decrease of the maximum horizontal load with the decrease in the unit strength, , is almost linear (-22% for the unit with f_c=15 N/mm^2, -45% for the unit with f_c=10 N/mm^2), even if for the unit with the lowest strength there is a small increase in the maximum displacement (+10%). In the case of the masonry specimens TG and Po, the decrease in the maximum horizontal load is lower for the unit with the highest strength (-11% when f_c=15 N/mm^2, -40% when f_c=10 N/mm^2), and similar for the two types of masonry. The behaviour in terms of maximum displacement is different for the two types of masonry: for the unit with the lowest strength there is an increase in the maximum displacement in the case of the masonry type TG (+27%), whereas there is always a decrease in displacement in the case of the masonry type Po (-45%), even if this can be due also to the overestimation of the experimental displacement in the original model.

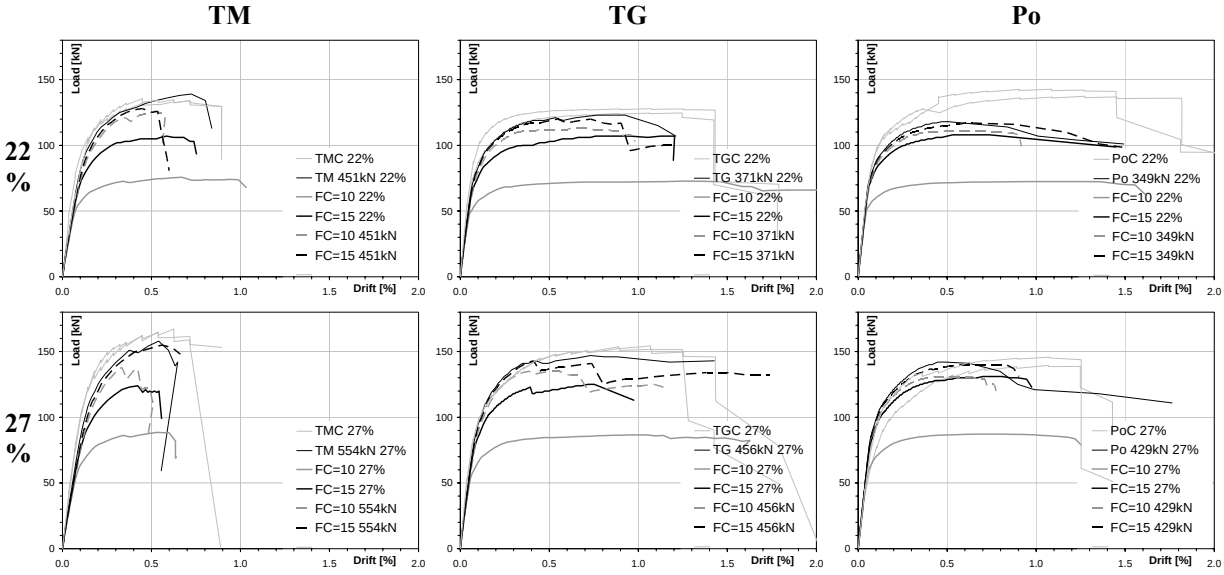

Figure 5. Load-drift diagrams. Experimental behaviour (grey), isotropic micro-model (black), masonry with f_{cu} = 15 N/mm^2 (blue) and f_{cu} = 10 N/mm^2 (red), under the same vertical load (dash line), under the same ratio of vertical load to compressive strength (full line).

CONCLUSIONS

An attempt was made of calibrating four different types of non-linear model on the basis of rigorous criteria. The analyses were carried out using the available experimental parameters, without arbitrary corrections. A criterion based on the net areas ratio was used to determine the orthotropic parameters from the isotropic ones. Also defined was a homogenization procedure that allows to source the micro-model parameters and to apply them into the analyses without any correction. The results showed that, in the case of the uniaxial compression, three out of four models are able to reproduce the experimental behaviour, and the orthotropic models seem to be more adequate. The experimental behaviour under diagonal compression can be described properly only by means of the interface models, whether they are orthotropic or isotropic. Besides, only the isotropic models adequately describe the shear compression tests. The accuracy of the models is influenced by the type of tests that is being simulated more than by the masonry type itself. In general, it can be said that any type of test can be well simulated by at least one type of modelling strategy.
The parametric analyses carried out on the shear behaviour of the three masonry typologies allowed defining the behaviour of masonry with different unit strength. The masonry made with thin layer joints (TM), shows a linear decrease of maximum horizontal load with the unit strength, and no or small increase of displacement capacity. In the case of masonry with ordinary bed joints (TG and Po), the maximum horizontal load shows a lower decrease in the case of the unit with the highest strength (-11%) and, at least for the units TG, there is an increase in the maximum displacement (+27%) for the unit with the lowest strength.

REFERENCES

da Porto F., E. Garbin, C. Modena, M.R. Valluzzi (2005). “Failure modes for in plane loaded masonry walls made with thin layer mortar” *10th Canadian Masonry Symposium*, Banff, Alberta, June 8 – 12, 2005, pp. 694-704
EN 1992-1-1 (2004) “Eurocode 2 - Design of concrete structures” - Part 1-1: General rules and rules for buildings
EN 1996-1-1 (2005) “Eurocode 6 - Design of masonry structures” - Part 1-1: General rules for reinforced and unreinforced masonry structures”
EN 1998-1 (2004) “Eurocode 8 - Design of structures for earthquake resistance” - Part 1: General rules, seismic actions and rules for buildings
Guidi G. (2006). “Sistemi di muratura portante in laterizio: calibrazione di modelli numerici sulla base di risultati sperimentali”. Graduation thesis, University of Padua (in Italian).
Lourenço P.B. (1996). “A user/programmer guide for the micro-modelling of masonry structures”, report no. 03-21-1-31-27, Delft University of Technology, The Netherlands.
Lourenço P.B., De Borst R., Rots J.G. (1997). “A plane stress softening plasticity model for orthotropic materials”, *International Journal of Numerical Methods in Engineering*, vol. 40, pp. 4033-4057
Lourenço P.B., Rots J.G. (1997). “A multi-surface interface model for the analysis of masonry structures”, *ASCE Journal of Mechanical Engineering*, vol. 123, no. 7, pp. 660-668
Mosele F. (2004). “Comportamento meccanico della muratura: Sperimentazione e modellazione”. Graduation thesis, University of Padua (in Italian).
Rots J.G. (1997). “Structural masonry an experimental/numerical basis for practical design rules”, Balkema, Rotterdam The Netherlands.
Tomaževič M., Lutman M., Bosiljkov V. (2006). “Robustness of hollow clay masonry units and seismic behaviour of masonry walls” Construction and Building Materials, vol. 20, n. 10, December 2006, pp. 1028–1039